

**LOS ANGELES-LONG BEACH HARBOR PIER 400  
HARBOR RESONANCE STUDY  
USING NUMERICAL MODEL, CGWAVE**

By

Dongcheng Li

B.S. Changsha Railway University, 1995

M.S. New Jersey Institute of Technology, 2002

A THESIS

Submitted in Partial Fulfillment of the

Requirements for the Degree of

Master of Science

(in Mechanical Engineering)

The Graduate School

The University of Maine

August, 2002

Advisory Committee:

Vijay G. Panchang, Professor of Marine Sciences, Advisor

Zeki Demirbilek, PE, Waterways Experiment Station

Vincent Caccese, Associate Professor of Mechanical Engineering

**LOS ANGELES-LONG BEACH HARBOR PIER 400**  
**HARBOR RESONANCE STUDY**  
**USING NUMERICAL MODEL, CGWAVE**

By Dongcheng Li

Thesis Advisor: Dr. Vijay Panchang

An Abstract of the Thesis Presented  
in Partial Fulfillment of the Requirements for the  
Degree of Master of Science  
(in Mechanical Engineering)  
August, 2002

Ports and harbors can be used for commercial, recreational and military purpose. Compared to other kinds of transportation (railroad, airplane, highways), waterborne commerce has two significant advantages: low cost and high capacity. Many nations use waterborne commerce as a major source of transport. Several major U.S. ports/harbors currently have renovation plans in response to the future expansion of ocean-borne world commerce, and coastal engineering projects generally require a detailed knowledge of the wave field in the project areas. Physical and numerical model studies are often conducted concurrently for these projects to evaluate technical feasibility and to optimize design alternatives. A coastal surface water wave model of the mild slope equation, CGWAVE is often used to predict waves since it is applicable to harbors, open coasts, inlets, around islands, and estuaries. The U.S. Army Corps Engineer Research and Development Center (ERDC, formerly WES) developed a physical model of Los Angeles and Long Beach harbors. It was utilized to simulate the propagation of both monochromatic and spectral waves in these harbors for assessing a range of wave periods

from several different directions. Data collected in that physical model study at locations of prototype gages were used to determine if the numerical model CGWAVE could reproduce observed measurements. This determination would help to make about future usage of CGWAVE model in prospects and to minimize expensive hydraulic model construction. Comparison between the results of numerical model predictions and actual wave heights measured at more than 50 wave gages is presented in this thesis.

## ACKNOWLEDGEMENTS

This study was supported by the Office of Naval Research, the Maine Sea Grant Program and the Army Corps of Engineer, of which I am greatly appreciative.

I wish to thank Professor Vijay Panchang for his time, effort and guidance throughout the course of my study. I also wish to thank Dr. Zeki Demirbilek for having made valuable suggestions and helped running the simulations. In addition, I would like to thank Professor Vicent Caccese and Professor Kewal K. Puri for their contributions.

Special thanks are extended to Mr. Karl Schlenker, for his continuous assistance on the use of SMS, and Dr. Wei Chen, who helped me understand the CGWAVE model. Finally, Mr. Liuzhi Zhao's support is acknowledged.

## TABLE OF CONTENTS

ACKNOWLEDGEMENTS.....	ii
LIST OF TABLES.....	iv
LIST OF FIGURES.....	v
Chapter	
1. INTRODUCTION.....	1
2. THE NUMERICAL MODEL CGWAVE.....	4
2.1. Fundamental Equations for CGWAVE.....	4
2.2. Boundary Conditions.....	9
2.2.1. Closed Boundary Conditions.....	9
2.2.2. Open Boundary Conditions.....	10
2.3. Numerical Solution.....	16
3. SUMMARY OF PHYSICAL MODEL LOS ANGELES-LONG BEACH HARBOR.....	20
4. SIMULATIONS IN THE LOS ANGELES-LONG BEACH HARBOR COMPLEX USING CGWAVE.....	26
5. CONCLUSION.....	44
REFERENCES.....	46
BIOGRAPHY OF THE AUTHOR.....	50

**LIST OF TABLES**

Table 1	Prototype Scaled Period Bands for Model Data.....	24
Table 2	Periods Used by Numerical Model for Long Waves.....	37

## LIST OF FIGURES

Figure 1. Los Angeles/Long Beach Harbor area, numbers show gage locations for hydraulic model study. (After Seabergh and Thomas, 1995).....	5
Figure 2. Harbor wave model domain; definition sketch.....	12
Figure 3. Two 1-d transects representing the exterior bathymetry .....	14
Figure 4. Data (Hydraulic Model) resonance curve at gage 6.....	21
Figure 5. Data (Hydraulic Model) resonance curve at gage 5.....	22
Figure 6. Bathymetry diagram for Los Angeles/Long Beach Harbor complex.....	27
Figure 7. Modeled phase diagram for Los Angeles/Long Beach Harbor complex, no reflection at coastal boundary, 50 second obliquely incident wave, with full breakwater.....	29
Figure 8. Wave height diagram for Los Angeles/Long Beach Harbor complex, no reflection, full breakwater, 50 second obliquely incident wave.....	30
Figure 9. Modeled phase diagram for Los Angeles/Long Beach Harbor complex, no reflection at coastal boundary, 100 second normal incident wave, without breakwater.....	31
Figure 10. Wave height comparison between numerical model (without breakwater) and hydraulic model results.....	32
Figure 11. Wave height comparison between numerical model (with full breakwater) and hydraulic model results.....	33

Figure 12. Diagram shows the full breakwater in the Los Angeles/Long Beach Harbor complex grid.....	35
Figure 13. Diagram shows the grid for Los Angeles/Long Beach Harbor complex with 50% breakwater permeable.....	36
Figure 14. Resonance curve comparison at gage 52 between Numerical Model and Data (Hydraulic Model).....	39
Figure 15. Resonance curve comparison at gage 53 between Numerical Model and Data (Hydraulic Model).....	40
Figure 16. Comparison between Numerical Model (CGWAVE) and Lab results.....	41
Figure 17. Resonance curve comparison at gage LB2 between Prototype and Data (Hydraulic Model).....	43

## Chapter 1

### INTRODUCTION

Because of its low cost and high capacity, waterborne commerce plays an important role in the economic growth and well-being of most nations. Ports and harbors are the center of waterborne transportation. They are important hubs for commercial, military, and recreational activities. For instance, about \$600 billion in foreign trade passed through ports in the United States in 1997; this trade is projected to triple by 2020 (YOTO, 1998). Engineers must provide the infrastructure that can handle this growth. Harbor facilities must accommodate ever-larger ships ("megaships") with increasingly demanding schedules and complex environmental regulations. It is therefore critical that these facilities be designed in a manner that enhances efficiency and safety of harbors operations such as cargo loading/unloading, etc.

Waves play a critical role, if not the most significant role, in all ocean-related activities. Waves damage shore protection structures, reshape beaches and affect shipping and navigation in inadequately protected harbors. One of the important features that can have an adverse impact on harbor operations is the wave climate. For example, some waves (not necessarily big waves) cause undesirable vessel motions (resulting in operational difficulties such as broken mooring lines, downtime for cargo handling, etc.) or undesirable sediment movement (resulting in more frequent dredging). Therefore, it is very necessary to understand the characteristics of nearshore waves. However, in most cases, little (if any) wave data are available for engineering construction and planning.

Field observation and physical modeling of waves are extremely difficult, costly and time-consuming. Furthermore, remote sensing instruments do not systematically provide the desired resolution in the near shore region and no data-recording instrument can anticipate or forecast future sea states. Therefore, the development of numerical wave models provides an effective method to obtain and evaluate the desired information for prospects.

In this thesis study, a numerical model (CGWAVE) is used to simulate surface water waves in Los Angeles-Long Beach Harbor, California, USA and the results are compared with the data obtained from measurements. CGWAVE model developed at the University of Maine, and is applicable to harbors, open coastal regions, and around islands. It is an efficient and easy-to-use wave model. The current version is user friendly and can provide the base wave information required for harbor/coastal prospects or offshore open sea applications. The model is tested herein using laboratory data obtained in a physical model of Los Angeles-Long Beach Harbor. This laboratory study was designed by the Army Corps Engineer Research & Development Center to investigate both monochromatic and spectral wave conditions in the harbor for a range of wave periods and directions. Since laboratory experiments can be carefully controlled for various wave parameters, they form a better test for a numerical model than field data. For example, field data may be influenced by wind or currents, which were not studied in the laboratory study.

While CGWAVE simulates the combined effects of wave refraction-diffraction included in the basic mild-slope equation, it also includes the effects of wave dissipation by friction, breaking, and nonlinear amplitude dispersion. It is a finite-element model that is interfaced with the Surface Water Modeling System (SMS) model (Jones & Richards, 1992) for graphics and efficient implementation (pre-processing and post-processing). CGWAVE has undergone several improvements in terms of iterative solution methods, boundary conditions, resolution, and some physical mechanisms compared to other models in this class.

The layout of this thesis is as follows. In chapter 2, a review of the numerical model CGWAVE is given. This is followed, in chapter 3, by some details about the physical model and laboratory data. CGWAVE results and the comparison between the laboratory data and the CGWAVE results are discussed in chapter 4. Concluding remarks are given in chapter 5.

## Chapter 2

### THE NUMERICAL MODEL CGWAVE

#### 2.1. Fundamental Equations for CGWAVE

Reliable estimation of wave conditions in and around a harbor is vital to the success of harbor operations. This estimation must often be accomplished through mathematical modeling techniques. However, most harbors confront the modeler with numerous complexities. Geometrically, as may be seen in Figure 1, the domain to be modeled may include completely arbitrary coastline shapes and bathymetric features, as well as man-made structures like piers, jetties, breakwaters, etc. These features induce wave refraction, diffraction, reflection, and dissipation by friction and breaking to varying degrees. The incident waves of interest may cover a wide spectrum, from very short waves to extremely long period waves that cause resonance, and may approach the harbor from any direction. For short waves, the number of grids needed to discretize the domain can be extremely large, making the modeling difficult. Longer waves may need fewer grids, but require a better specification of boundary reflectivity, because they are more susceptible to reflections in all directions from structures, coastlines, and bathymetric slopes. In addition to these complexities, the modeler may also have to account for the effects of the interaction between various wave components and tidal or other currents that can magnify or diminish the wave climate in different parts of the domain.

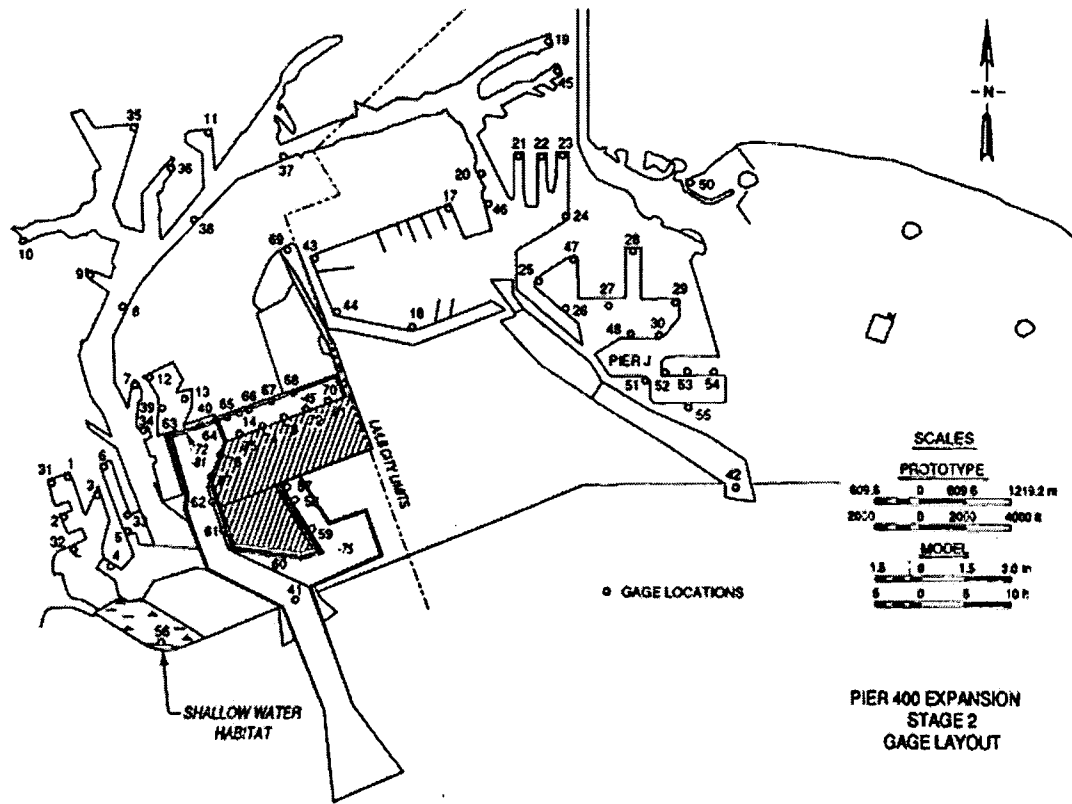


Figure 1. Los Angeles/Long Beach Harbor area, numbers show gage locations for hydraulic model study. (After Seabergh and Thomas, 1995)

In this paper, a methodology that has become well-accepted in recent years is summarized for modeling wave motion in harbors. See Panchang et al. 1999 for a review of recent coastal wave modeling methods. In its basic form, the methodology is based on solving the following two-dimensional elliptic equation:

$$\nabla \cdot (CC_g \nabla \phi) + k^2 CC_g \phi = 0 \quad (1)$$

where

- $\phi(x,y)$  = complex surface elevation function ( $=\phi_1 + i\phi_2$ )
- $i$  =  $\sqrt{-1}$
- $\sigma$  = wave frequency under consideration
- $C(x,y)$  = phase velocity =  $\sigma/k$
- $C_g(x,y)$  = group velocity =  $\partial\sigma/\partial k$
- $k(x,y)$  = wavenumber ( $= 2\pi/L$ ), related to the local depth  $d(x,y)$  through the dispersion relation:

$$\sigma^2 = gk \tanh(kd). \quad (2)$$

The wave height  $H$  can be obtained from complex surface elevation function  $\phi$  as follows:

$$H = \frac{2\sigma}{g} \sqrt{(\phi_1^2 + \phi_2^2)} \quad (3)$$

Essentially (1) represents integration over the water column of the three-dimensional Laplace equation used in potential wave theory. The integration, originally described by Berkhoff (1976) and Smith and Sprinks (1975), is necessary because the solution of the three-dimensional problem is computationally difficult for harbors with a characteristic length that is several times the wavelength. The integration is based on the assumption that the vertical variation of the wave potential is largely the same as that for a horizontal bottom, i.e.

$$\phi(x, y, z) \approx \frac{\cosh k(d+z)}{\cosh kd} \phi(x, y) \quad (4)$$

This approximation is obviously valid for a "mild slope", characterized by  $|\nabla d|/kd \ll 1$ , a criterion that is usually met in practice. Being elliptic, (1) represents a boundary value problem which can accommodate internal nonhomogeneities. It hence forms a widely-used basis for performing wave simulations in regions with arbitrarily-shaped (manmade or natural) boundaries and arbitrary depth variations. Unlike "approximate" mild slope wave models (e.g. REFDIF and RCPWAVE described by Dalrymple et al. 1984; Kirby, 1986; and Ebersole, 1985), there are no intrinsic limitations on the shape of the domain, the angle of wave incidence, or the degree and direction of wave reflection and scattering that can be modeled with (1).

In essence, (1) represents the complete two-dimensional wave scattering problem for the non-homogeneous Helmholtz equation, as demonstrated by Radder (1979). While it is valid for a monochromatic (single incident frequency-direction) wave condition, irregular wave conditions may be simulated using (1) by superposition of monochromatic simulations.

For further development, we may consider the following extended form of (1):

$$\nabla \cdot (CC_g \nabla \phi) + (k^2 CC_g + iC_g \sigma W) \phi = 0 \quad (5)$$

in which a dissipation term  $W$  has been included. By separating the real and imaginary parts of (5), Booij (1981) has shown that (5) satisfies the energy balance equation in the presence of dissipation. The term  $W$  may represent breaking and/or friction and is described later.

Several computational models based on (1) or (5) have been developed in recent years (e.g. HARBD, PHAROS, RCPWAVE etc.). These models differ in the choice of the numerical method used (e.g. finite-difference method, boundary element method, finite element method), in the choice of boundary conditions, in the method used to solve the linear system of equations that results from discretizing the elliptical governing equation, and in the inclusion of additional mechanisms. While a detailed comparison of the models is outside of the scope of this thesis, here a brief summary of these features is provided as they pertain to CGWAVE. For a detailed review and comparison of models, see Panchang and Demirbilek (2001).

## 2.2. Boundary Conditions

Domains on which the elliptic eq. (5) is solved are enclosed by closed boundaries (represented by coastlines and surface-penetrating structures like pier walls or pier legs, breakwaters, seawalls, etc.) and open boundaries (which represent an artificial boundary between the area being modeled and the sea region outside). A separation between the model domain and an outer water area from where no waves enter the model domain (e.g. a creek or tributary at the back bay or down wave end of the domain) may be considered to be a fully-absorbing closed boundary. An open boundary is considered to be one where an incident wave is specified (and may contain other radiated waves). Along all boundaries, appropriate conditions must be specified to solve (1); however, even in the best of circumstances, only approximate boundary conditions can be developed (e.g. see Dingemaans, 1997).

### 2.2.1. Closed Boundary Conditions

Along coastline and surface-protruding structures, the following boundary condition has traditionally been used (e.g. Berkhoff 1976; Tsay & Liu 1983; Tsay et al. 1989; Oliveira and Anastasiou 1998; Li 1994a)

$$\frac{\partial \phi}{\partial n} = \alpha \phi \quad (6)$$

where  $n$  is the outward normal to the boundary and  $\alpha$  is related to a user-specified reflection coefficient as follows:

$$\alpha = ik \frac{1 - K_r}{1 + K_r} \quad (7)$$

$K_r$  varies between 0 and 1 and specific values for different types of reflecting

surfaces have been compiled by Thompson et al. (1996). Here we used a version of CGWAVE that was linear in  $Kr$ , i.e. the reflection coefficient not depends on the incident wave angle, for details about closed boundary reviews, please refer to Panchang & Demirbilek (2001).

### 2.2.2 Open Boundary Conditions

Along the open boundary, an incident wave  $\phi_i$  must be specified. Along this boundary, however, waves backscattered from within the domain will also exist, and their magnitude is generally not known. In the context of simple rectangular domain models, with one side (aligned, say, in the  $y$  direction) constituting the open boundary, Panchang et al. (1988, 1991), Li (1994a, b), and Oliveira and Anastasiou (1998) have used the following condition

$$\frac{\partial \phi}{\partial x} = ik(2\phi_i - \phi) \quad (8)$$

(8) is obtained by assuming that the incident and backscattered components along this boundary can be described by  $\phi_i = A_i \exp(ikx)$  and  $\phi_b = B \exp(-ikx)$  respectively (where  $A_i$  is the (specified) amplitude of the incoming wave and  $B$  is an unknown), adding the two components, and differentiating. Obviously, this is valid only if the incident and backscattered waves near the boundary are plane waves propagating in the  $\pm x$  direction.

For more complex domains involving multidirectional scattering, (8) is inappropriate. Harbor applications generally use model domains such as that

described in Figure 2, where the semicircle is used to separate the model area from the open sea. In the exterior domain  $\Omega'$  the potential  $\phi$  is comprised of three components:

$$\phi = \phi_i + \phi_r + \phi_s \quad (9)$$

where  $\phi_i$  = the incident wave that must be specified to force the model,  $\phi_r$  = a reflected wave that would exist in the absence of the harbor, and  $\phi_s$  = a scattered wave that emanates as a consequence of the harbor and must satisfy the Sommerfeld radiation condition. With appropriate descriptions for these components, a boundary condition can be developed along the semicircle.

An effective way to describe the exterior wave conditions is to use a “parabolic approximation” to describe  $\phi_s$ :

$$\frac{\partial \phi_s}{\partial n} = -p\phi_s - q \frac{\partial^2 \phi_s}{\partial \theta^2} \quad (10)$$

where

$$p = -ik_0 + \frac{1}{2r} - \frac{i}{8k_0 r^2}, \quad q = -\frac{i}{2k_0 r^2} \quad (10a)$$

where  $r$  and  $\theta$  represent the polar coordinates of a point on the open boundary and  $k_0$  is a representative wavenumber for the open boundary. ( $p$  and  $q$  are not unique, and alternative forms, each obtained with an appropriate rationale, have been investigated by Givoli (1991), Xu et al. (1996), Panchang et al. (2000)). The parabolic approximation (10) allows the scattered waves to exit only through a

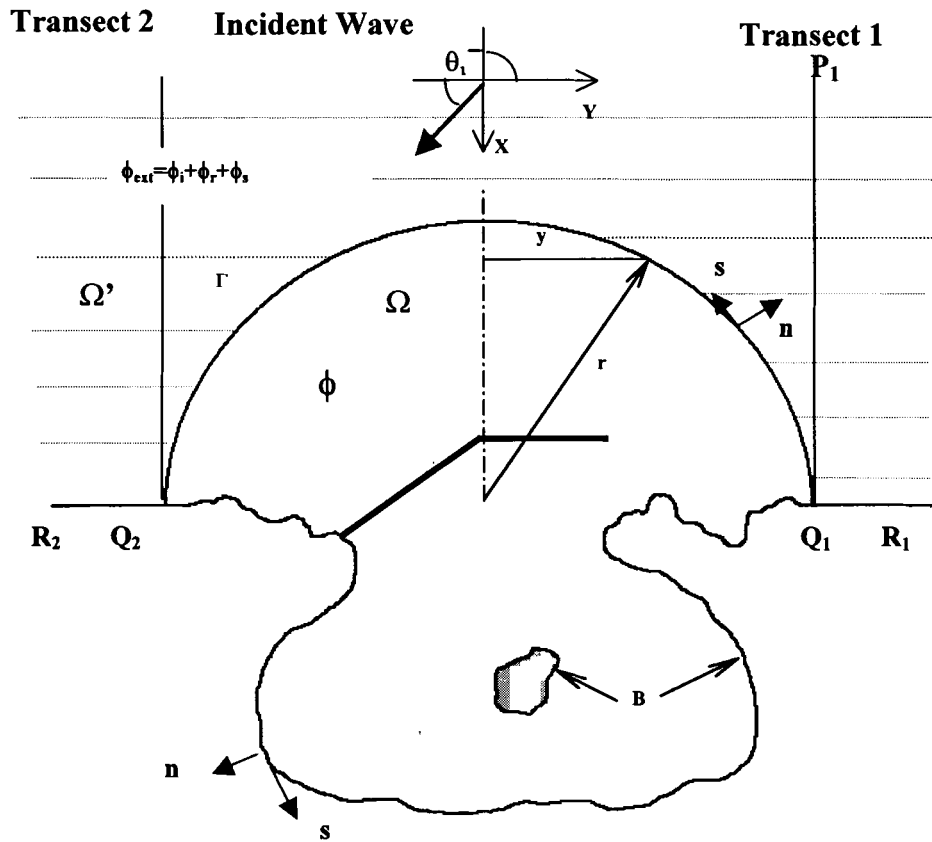


Figure 2 . Harbor wave model domain; definition sketch.

limited aperture around the radial direction. Unlike (9), therefore, it does not rigorously satisfy the Sommerfeld radiation condition. However, using this formulation decouples  $\phi_s$  from the other components. These components ( $\phi_1$  and  $\phi_2$ ) may be obtained by making a compromise between a detailed exterior bathymetric representation (which is difficult) and the constant depth representation (which is used in older models like HARBD). A one-dimensional representation, where the depths vary in the cross-shore direction only (Figures 2, 3), may be selected. This is reasonable, since in general, this is often the direction in which the depths vary the most. If natural variations do not permit the representation of the exterior depths by only one section, a second one-dimensional section, shown as transect 2 in Figures. 3 and 4, may be constructed. For transects 1 and 2 with varying depths, no simple analytical expression can be found for the reflected wave (since  $\phi_1$  and  $\phi_2$  are coupled). However, the quantity:

$$\phi_0 = \phi_1 + \phi_2 \quad (11)$$

may be obtained by the solution of the one-dimensional version of (5), since the depths along these transects vary in one direction only. This one-dimensional equation is (Panchang et al. 2000):

$$\frac{d}{dx} (CC_g \frac{d\psi}{dx}) + kCC_g(k\cos^2\theta + iW) \psi = 0 \quad (12)$$

where, for one-dimensional geometry,

$$\phi_0 = \psi(x) \exp(iky \sin\theta) \quad (13)$$

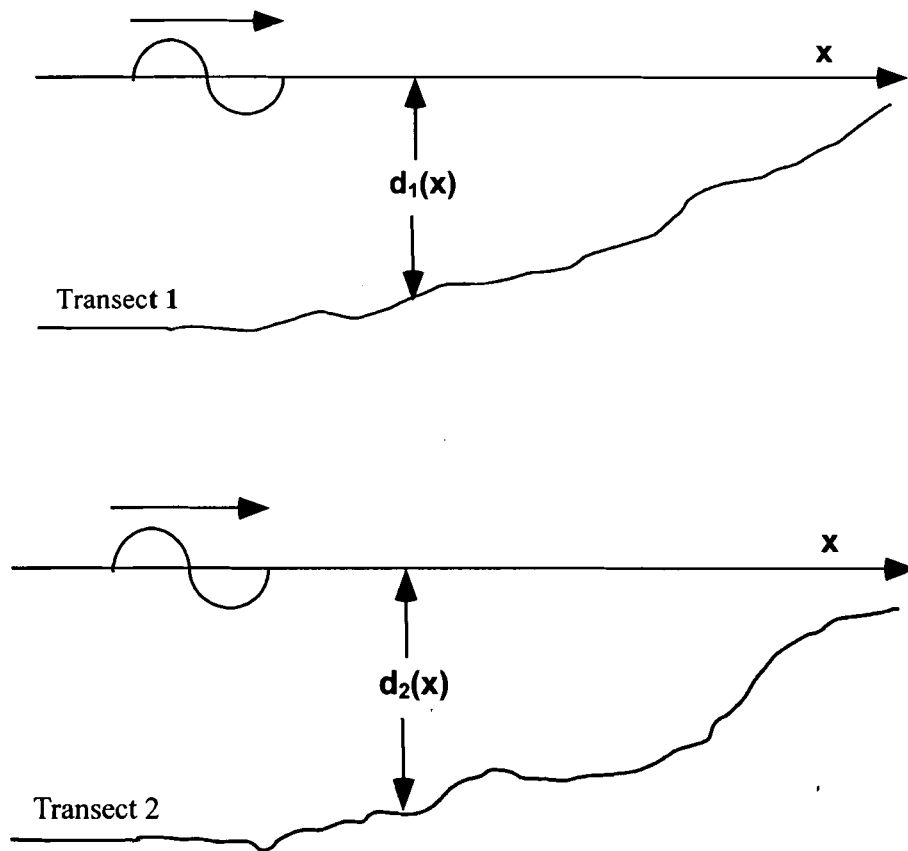


Figure 3. Two 1-d transects representing the exterior bathymetry (do not have to be identical).

(13) is an elliptic ordinary differential equation requiring two boundary conditions. It may easily be solved via a simple finite-difference scheme. (For the present, the dissipation factor  $W$  is considered to be prespecified). Assuming that transect 1 extends out to a region of constant depth (or deep water), a condition at  $P_1$  may be obtained by combining a specified incident wave

$$\phi(P_1) = A_i \exp(ikx \cos\theta_i +iky \sin\theta_i) \quad (14)$$

(where  $A_i$  = a given input wave amplitude) and an unknown reflected wave:

$$\phi(P_1) = B \exp(-ikx \cos\theta_i +iky \sin\theta_i) \quad (15)$$

Without loss of generality, the point  $P_1$  may be located at  $x = 0$ , which allows elimination of  $B$  to yield

$$\frac{\partial\psi}{\partial x} = ik\cos\theta_i(2A_i - \psi) \quad (16)$$

At the coastal boundary point  $Q_1$ , the partial reflection boundary condition (9) may be used in the following form:

$$\frac{\partial\psi}{\partial x} = \frac{i\sqrt{k^2 - k^2\sin^2\theta}(1 - K_r)}{1 + K_r} \psi \quad (17)$$

Where  $K_r$  is the reflection coefficient for the exterior coastline (i.e. near  $Q_1$ ) and  $k\sin\theta$  is constant for the one-dimensional problem.

The solution of (12) using boundary conditions (16) and (17) along with (13) produces  $\phi_0$  along transects 1 and 2. These solutions are denoted by  $\phi_{01}$  and  $\phi_{02}$ . The desired  $\phi_0$  along the semicircle may be obtained by laterally translating  $\phi_{01}$  and  $\phi_{02}$  via interpolation between transects 1 and 2 as follows:

$$\phi_0 = (1 - m) \phi_{01} \exp(-ik(r-y)\sin\theta) + m \phi_{02} \exp(ik(r+y)\sin\theta) \quad (18)$$

Where we have set  $y = 0$  at the center of semicircle, the interpolation function  $m = (r-y)/2r$ ,  $r$  is the radius of the semicircle,  $y$  is the lateral coordinate of the open boundary node relative to the origin of semicircle (Figure 3).

### 2.3. Numerical Solution

Equation (5) is generally solved using the boundary element method, the finite-difference method, or the finite element method. In general, finite-difference discretizations are not well-suited to represent the complex domain shapes described, for example, in Figure 1. Not only are the boundaries distorted, but the number of uniformly spaced grids may also be excessively large. (Adequate resolution, typically 10 points per wavelength, demands that the spacing be determined from the smallest wavelength.) Most studies with the finite-difference method have been limited to largely rectangular domains (e.g. Li 1994a, 1994b; Panchang et al. 1991; Li and Anastasiou 1992). Boundary element models can handle arbitrary shapes and require minimal storage since only the boundaries are discretized; however, they are limited to subdomains with constant depths only (e.g. Isaacson and Qu 1990; Lee

and Raichlen 1972; Lennon et al. 1982). Finite element models, on the other hand, allow the construction of grids with variable sizes (based on the local wavelength) and give a good reproduction of the boundary shapes. Like most finite element models (e.g. Tsay and Liu 1983; Tsay et al. 1989; Kostense et al. 1988), CGWAVE uses triangular elements, but it is also interfaced to modern graphical grid generating software that permits efficient and accurate representation of harbors with complex shapes. This software, called the Surface Water Modelling System (Zundell et al. (1998); and Jones and Richards (1992)) can be used to conveniently generate as many as 500,000 elements of varying size, based on the desired (user-specified) resolution, and to specify the desired reflection coefficients on various segments of the closed boundary.

The numerical treatment of (1) with appropriately chosen boundary conditions leads to system of linear equations:

$$[A] [\phi] = [B] \quad (19)$$

where  $[\phi]$  represents the vector of all the unknown potentials. For solving (5), a similar system results as long as  $W$  is prespecified. The matrix  $[A]$  is usually extremely large. In earlier models (e.g. Tsay and Liu 1983; Tsay et al. 1989; Chen, 1990; Chen and Houston, 1987) the solution of (19) was accomplished by Gaussian Elimination, which requires enormous memory and is prohibitive when the number of wavelengths in the domain is large (i.e. short waves or a large domain).

In CGWAVE, the solution of (19) has been obtained with minimal storage

requirements for [A]. This is due to the development by Panchang et al. (1991) and Li (1994a) of iterative techniques especially suited for (1). These techniques, based on the conjugate gradient method, guarantee convergence and have been found to be extremely robust in a wide variety of applications involving both finite differences and finite elements for several kinds of boundary conditions. More recently, Oliveira and Anastasiou (1998) explored the use of the Generalized Minimum Residual method and the Stabilized Biconjugate Gradient method and reported greater efficiency with finite-difference models based on (1). With a finite-element formulation, however, Zhao et al. (2000) found that the GMRES method of Oliveira and Anastasiou (1998) failed to converge whereas their latter method yielded erratic efficiency.

For modeling spectral wave conditions, the input spectrum is discretized into several components, and each component is modeled by methods described above. The solution (or significant wave height) any grid point is calculated by linear superposition. For this study, a spectral version was used in which significant improvements in speed were obtained by using two-level code parallelization for operation on high performance parallel computing platforms such as the SGI/Cray Origin2000 (O2K). For spectral simulations without interfrequency exchange, the solution of (1) for each monochromatic component leads to an independent system of linear equations. These equations are solved using distributed clusters of shared-memory multiprocessors (SMPs), which have to communicate and share the workload, e.g. via a Message Passing Interface, MPI. Individual wave components

are distributed to multiple processors via MPI and load-balanced through the Manager-Worker model (Foster 1997; Bova et al. 2000). At the second level, matrix operations are parallelized, since most of the CPU-time for each wave component is utilized in the solution of the linear system of equations. For conjugate gradient solvers, 90% of the CPU time is spent on matrix-vector products and inner product kernels. Therefore, OpenMP (OARB 1997) may be used to parallelize the kernels. Two-level parallelization schemes can use OpenMP to accelerate the solution for each component and MPI to simultaneously obtain solutions to multiple incident wave components. More details regarding parallelization schemes for harbor wave models may be found in Bova et al. (2000), who report a reduction in run times by a factor of 250-580 compared with serial codes for an application in Ponce de Leon Inlet (Florida). A problem with nearly 300 input spectral components was solved on a 25 sq. km domain containing 235,000 nodes in 72 hours. With the recent developed super-fast solvers, the run time for this problem has been lowered to 3 hours. This fast version was available on the DOD supercomputer at the Army R & D center.

### Chapter 3

## SUMMARY OF PHYSICAL MODEL LOS ANGELES-LONG

### BEACH HARBOR

The Army Corps of Engineers developed a physical model of Los Angeles-Long Beach Harbor located at Army R & D Center in Vicksburg, Mississippi. The model was molded in concrete grout at a vertical scale of 1:100 and a horizontal scale of 1:400 and reproduced San Pedro Bay and the Pacific Ocean seaward of the harbor out to the 91.44 m (300 feet) mllw, contour. The model shoreline extended from 3.2km (2 miles) northwest of Point Fermin to Huntington Beach. The total area reproduced in the model covered about 474 sq m (44,000 sq ft), representing 655 sq km (253 square miles) in the prototype. It is described in detail by Seabergh and Thomas (1995).

The model was originally constructed to conditions as they existed in the early 1970's and has been periodically updated. For this work, care was taken to ensure that the latest bathymetry and harbor geometry was in place. The "Long Beach Harbor Pier J Expansion" and projected increased channel depths, which were completed in 1990, also were included in the definition of existing harbor layout. Plans for Stage 1 and 2 were provided by the Los Angeles District and the Port of Los Angeles. Seabergh and Thomas (1995) conducted hydraulic model simulations. As noted earlier, they collected data at several gages, shown in Fig.1, for various harbor plans. However, the detailed hydraulic model bathymetry was not available to us; hence we used the bathymetry from the latest NOAA chart (18749). The

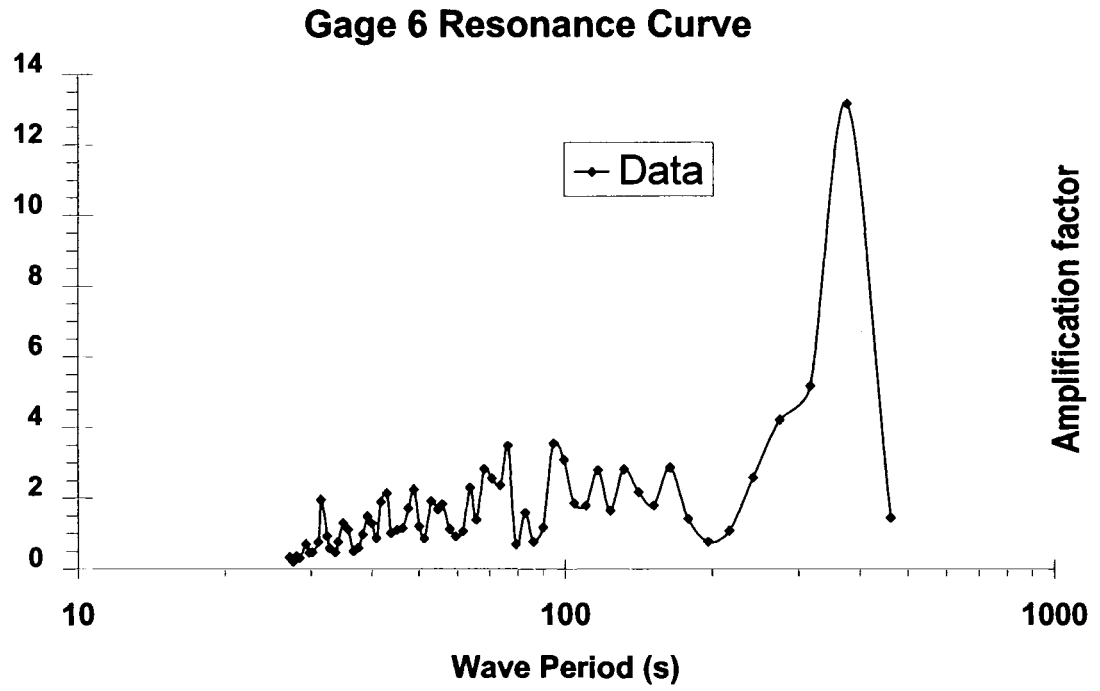


Figure 4. Data (Hydraulic Model) resonance curve at gage 6.

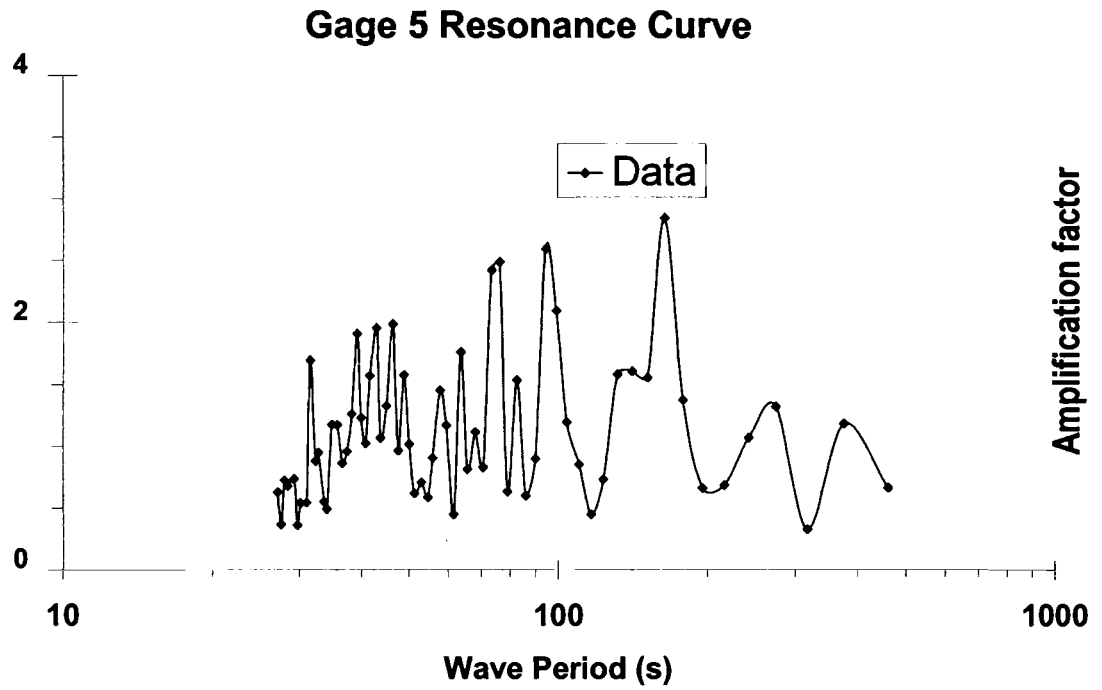


Figure 5. Data (Hydraulic Model) resonance curve at gage 5.

bathymetric data used for numerical modeling obtained from this recent NOAA chart was a reasonable approximation of the harbor geometry described as “stage II” by Seabergh and Thomas (1995). However, neither the bathymetry data nor the boundary geometries used in the two studies were identical.

Seabergh and Thomas (1995) conducted hydraulic model simulations and collected data at several gages (Fig. 1). Comparison between the results of hydraulic model and actual wave heights collected by the wave gages have been done and discussed. They performed their hydraulic model experiments for a large number of input frequency components varying from 30 seconds to 512 seconds. The periods they used for experiments are listed in the table 1. At each gage location, the amplification factor was measured for several frequencies and a resonance curve was developed. These curves were found to be extremely noisy, i.e., the response varied quite rapidly with frequency at the gages (see example in Fig.4, Fig.5, Fig.14 and Fig.15). For convenience of analysis, therefore, they partitioned the data into three groups: short period waves (30 s to 42 s), medium period waves (42 s to 205 s) and long period waves (205 s to 512 s). All the periods they used for their experiments are shown in Table 1. For each gage, the amplification factors within each group were averaged over the respective frequencies.

Prototype Scaled Period Bands for Model Data		
period band	Frequency-cps	Period Range
30.37	0.032927	30.1-30.6
30.83	0.032436	30.6-31.1
31.3	0.031949	31.1-31.5
31.78	0.031466	31.5-32.0
32.28	0.030979	32.0-32.5
32.8	0.030488	32.5-33.1
33.33	0.030003	33.1-33.6
33.89	0.029507	33.6-34.2
34.46	0.029019	34.2-34.8
35.05	0.028531	34.8-35.4
35.56	0.028121	35.4-36.0
36.29	0.027556	36.0-36.6
36.94	0.027071	36.6-37.3
37.62	0.026582	37.3-38.0
38.83	0.025753	38.0-38.7
39.06	0.025602	38.7-39.4
39.82	0.025113	39.4-40.2
40.6	0.024631	40.2-41.0
41.43	0.024137	41.0-41.8
42.28	0.023652	41.8-42.7
43.17	0.023164	42.7-43.6
44.1	0.022676	43.6-44.6
45.07	0.022188	44.6-45.6
46.09	0.021697	45.6-46.6
47.15	0.021209	46.6-47.7
48.26	0.020721	47.7-48.8
49.42	0.020235	48.8-50.0
50.65	0.019743	50.0-51.3
51.93	0.019257	51.3-52.6
53.28	0.018769	52.6-54.0
54.7	0.018282	54.0-55.4
56.21	0.01779	55.4-57.0
57.79	0.017304	57.0-58.6
59.74	0.016739	58.6-60.3
61.25	0.016327	60.3-62.2
63.14	0.015838	62.2-64.1
65.15	0.015349	64.1-66.2

Table 1. Prototype Scaled Period Bands for Model Data.

Prototype Scaled Period Bands for Model Data		
period band	Frequency-cps	Period Range
67.29	0.014861	66.2-68.4
69.57	0.014374	68.4-70.8
72.02	0.013885	70.8-73.3
74.64	0.013398	73.3-76.0
77.47	0.012908	76.0-79.0
80.51	0.012421	79.0-82.1
83.81	0.011932	82.1-85.6
87.38	0.011444	85.6-89.3
91.28	0.010955	89.3-93.3
95.53	0.010468	93.3-97.8
100.21	0.009979	97.8-102.7
105.36	0.009491	102.7-108.2
111.08	0.009003	108.2-114.2
117.45	0.008514	114.2-121.0
124.59	0.008026	121.0-128.5
132.66	0.007538	128.5-137.1
141.85	0.00705	137.1-147.0
152.41	0.006561	147.0-158.4
163.66	0.00611	158.4-171.7
179.06	0.005585	171.7-187.4
196.22	0.005096	187.4-206.0
217.01	0.004608	206.0-229.1
242.73	0.00412	229.1-258.1
275.36	0.003632	258.1-295.4
318.14	0.003143	295.4-354.4
376.64	0.002655	354.2-414.1
461.52	0.002167	414.1-519.5

Table 1. Prototype Scaled Period Bands for Model Data.

## Chapter 4

### SIMULATIONS IN THE LOS ANGELES-LONG BEACH HARBOR COMPLEX USING CGWAVE

The Los Angeles/Long Beach Harbor complex (Figure 1) is one of the largest harbors in the world; therefore, the model domain is quite large covering an area of approximately 120 square km. The Surface Water Modeling System (Zundel et al. 1998) was used for grid generation. Bathymetric input (Figure 6) was obtained by digitizing NOAA chart number 18749. For numerical modeling, a grid containing 285,205 triangular finite elements was developed. It was based on a resolution of 10 points per wavelength for a 30-second wave. We use the 30-second wave as the benchmark to make the grid, because the 30-second wave is the shortest period wave we modeled, the resolution requirements will be satisfied for all the other longer period waves. The two one-dimensional transects in the exterior were extended in the offshore direction to a distance of 9.2 km, beyond which the depth was assumed to be constant; this distance of 9.2 km is longer than the radius of the open boundary. At this location, the input wave for the numerical model was specified.

For initial quality control simulations, the coastal reflectivity was set equal to zero (i.e., fully absorbing) since this case is easier to examine qualitatively than the case when a large number of reflections are present, the offshore breakwater reflectivity was set equal to 0.1. Figure 7 shows the phase diagram for a 50 second obliquely incident wave. The results appear to be quite satisfactory. A reduction in

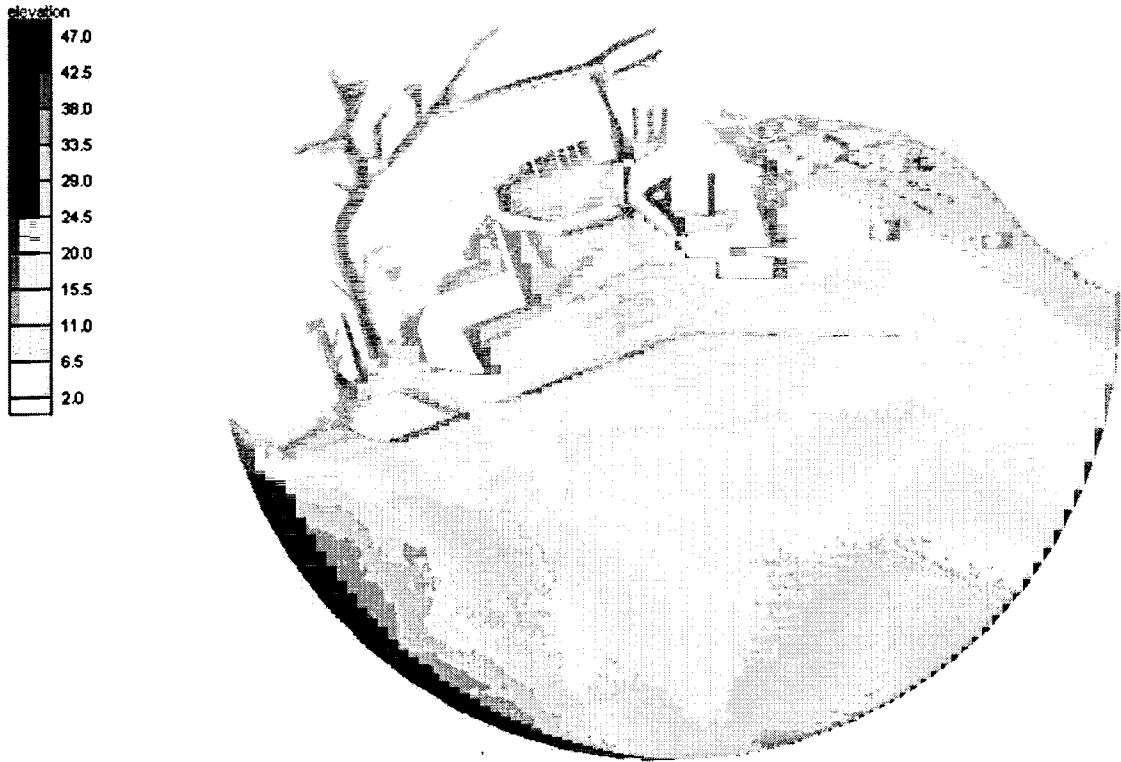


Figure 6. Bathymetry diagram for Los Angeles/Long Beach Harbor complex.

the wavelength in the onshore direction is evident. No spurious boundary effects are seen. Penetration through the breakwater gaps is precisely as one would expect. Bending of the crests as they approach from on shore also indicates a correct reproduction of refractive effects. Figure 8 shows the wave heights diagram for this same 50 second obliquely incident wave, as one expected, the wave heights are significantly reduced after the wave go through the breakwater, penetration through the breakwater gaps is obvious. Figure 9 shows the phase diagram for a 100 second normal incident wave, in this case, the offshore breakwater showed in Figure 3 is taken off. The results of this case are quite satisfactory too. The wavelength is clearly longer than in Fig.3

For further simulations, the coastal boundary was assumed to be fully reflecting (both inside the model and for the one-dimensional transects), the offshore breakwater reflectivity still was set equal to 0.1. Also, the offshore breakwaters are known to be permeable to waves (e.g., Chiang, 1988) and it is hence not appropriate to consider them as closed boundaries. In order to examine it, the numerical simulations were made with the full offshore breakwater. Figure 11 shows the comparison for long period waves (205 s to 512s) between the numerical simulation and hydraulic model results, the numerical simulation is based on the bathymetric data with a full offshore breakwater. At almost all gage locations, the model results are highly underpredicted. I also made another set of simulations for a bathymetry without offshore breakwater. Figure 10 shows the comparison for long period waves (205 s to 512s) between the numerical simulation and hydraulic model results,



Figure 7. Modeled phase diagram for Los Angeles/Long Beach Harbor complex, no reflection at coastal boundary, 50 second obliquely incident wave, with full breakwater.

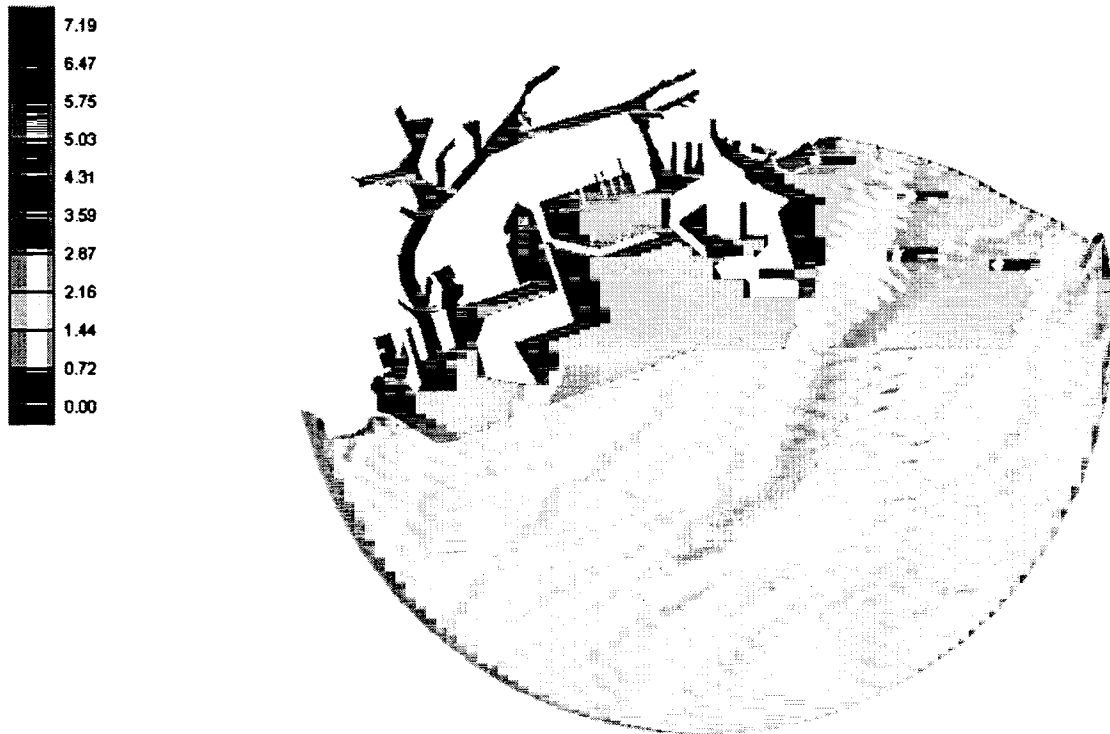


Figure 8. Wave height diagram for Los Angeles/Long Beach Harbor complex, no reflection, full breakwater, 50 second obliquely incident wave.

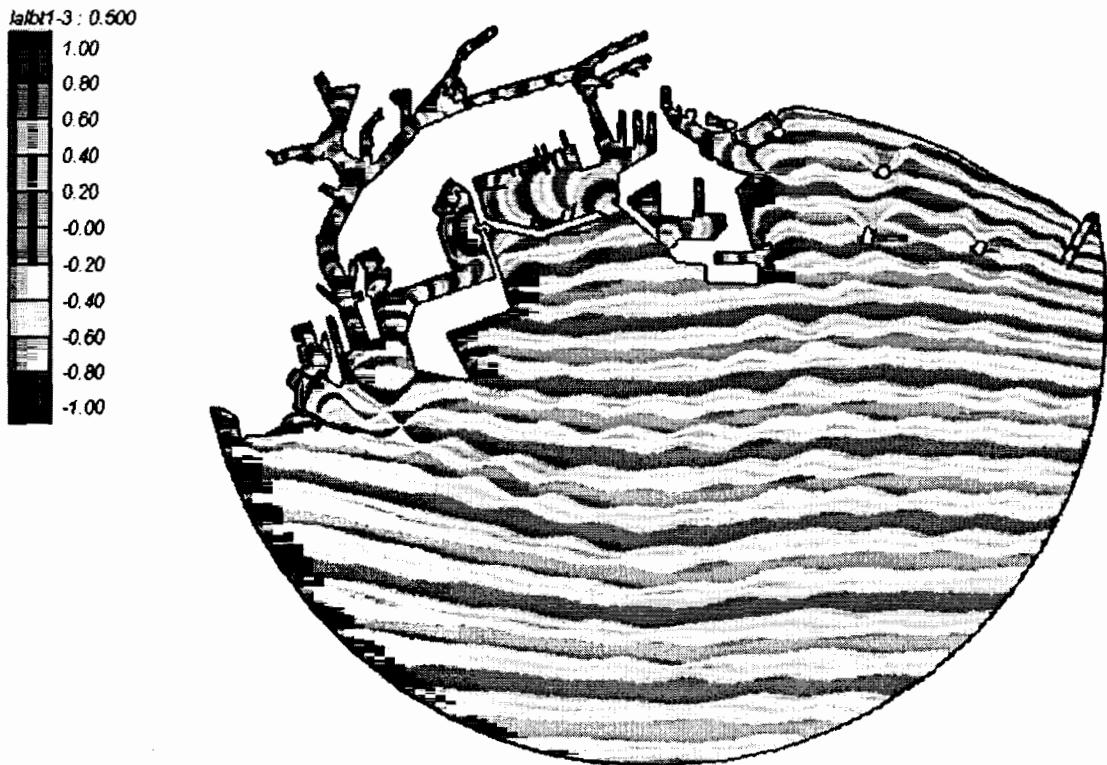


Figure 9. Modeled phase diagram for Los Angeles/Long Beach Harbor complex, no reflection at coastal boundary, 100 second normal incident wave, without breakwater.

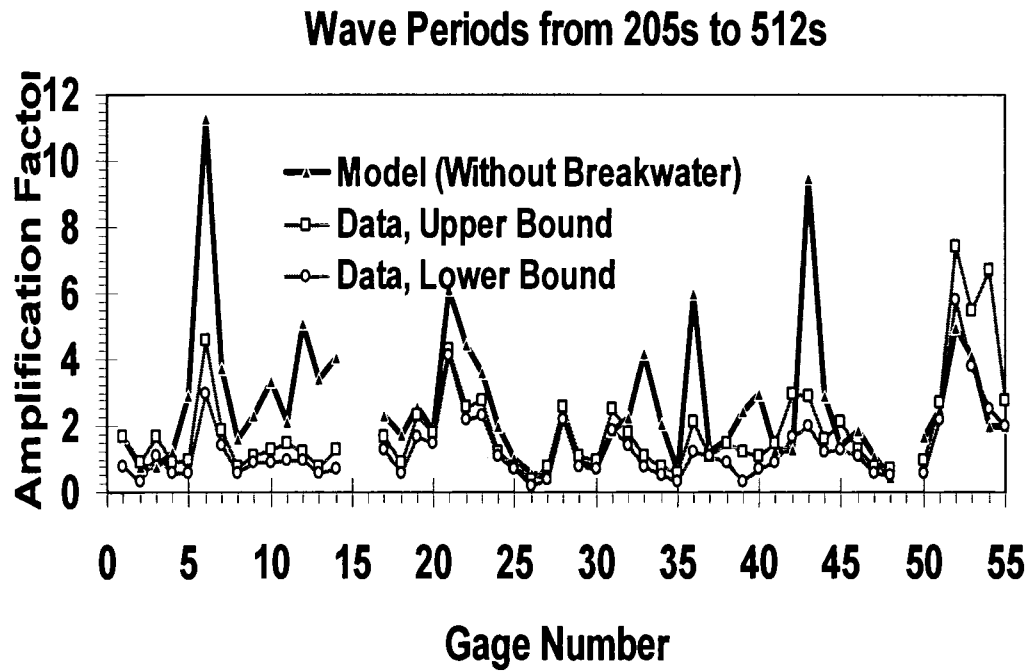


Figure 10. Wave height comparison between numerical model (without breakwater) and hydraulic model results.

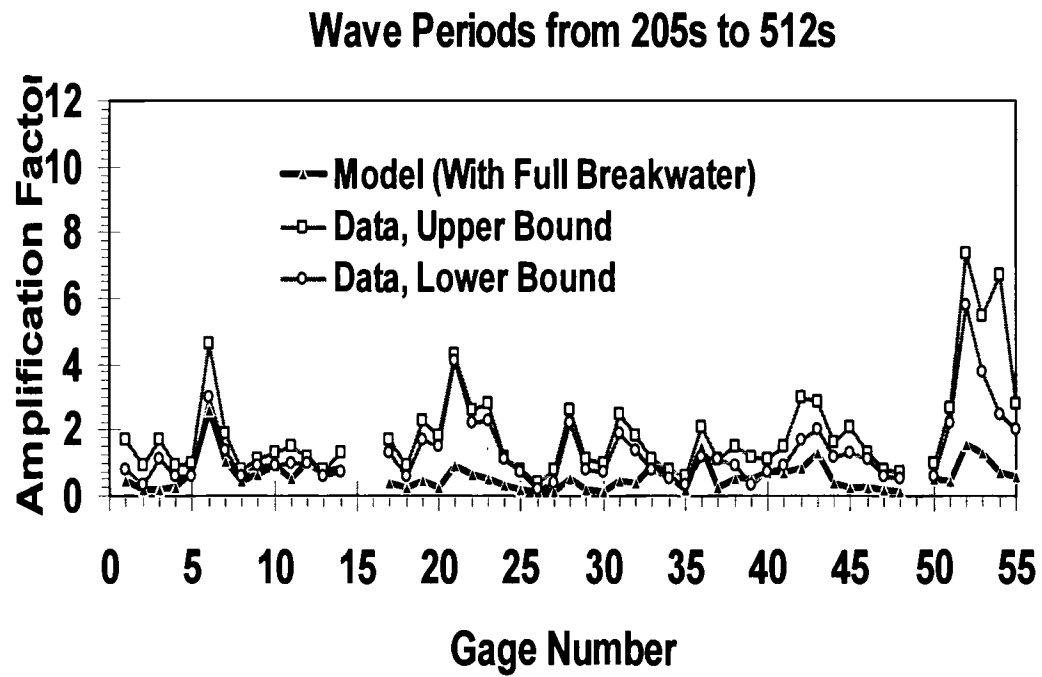


Figure 11. Wave height comparison between numerical model (with full breakwater) and hydraulic model results.

clearly, too much energy enters the harbor area. At almost all gage locations, the model results are overpredicted. Permeable structures cannot be easily handled within the context of an elliptic boundary value problem. One approach may be to treat the breakwater as a water area and ascribe an appropriate dissipation factor in that region. I used an alternative approach whereby the breakwater was divided into several segments so that energy could propagate through gaps in the breakwater. After much experimentation, a decision was made to take 50% of the offshore breakwater off by means of numerous gaps interspersed among several solid segments, the results will be discussed later. Figures 12 and 13 depict a part of the Los Angeles/Long Beach complex grid, with the full breakwater and 50% open. In the process of taking off part of the breakwaters, a large number of small segments as opposed to a small number of long segments were attempted. This was done to simulate uniform permeability. Otherwise, this approach would interfere solutions immediately behind certain segments and hence the comparison at gages in their vicinity. The segmentation was done with due consideration of gage locations and practicality of grid generation. In total, 36 segments were used, with average segment of 140 meters long.

Numerical simulations were performed for three incident angles, for normal incidence and for  $30^\circ$  on either side of it, to account for the effects of the wave maker. The results of the three directional inputs were averaged for each frequency. The exact location of each gage was not known, so results in the general vicinity of the gage as determined from Figure 1 were extracted and averaged over the



Figure 12. Diagram shows the full breakwater in the Los Angeles/Long Beach Harbor complex grid.

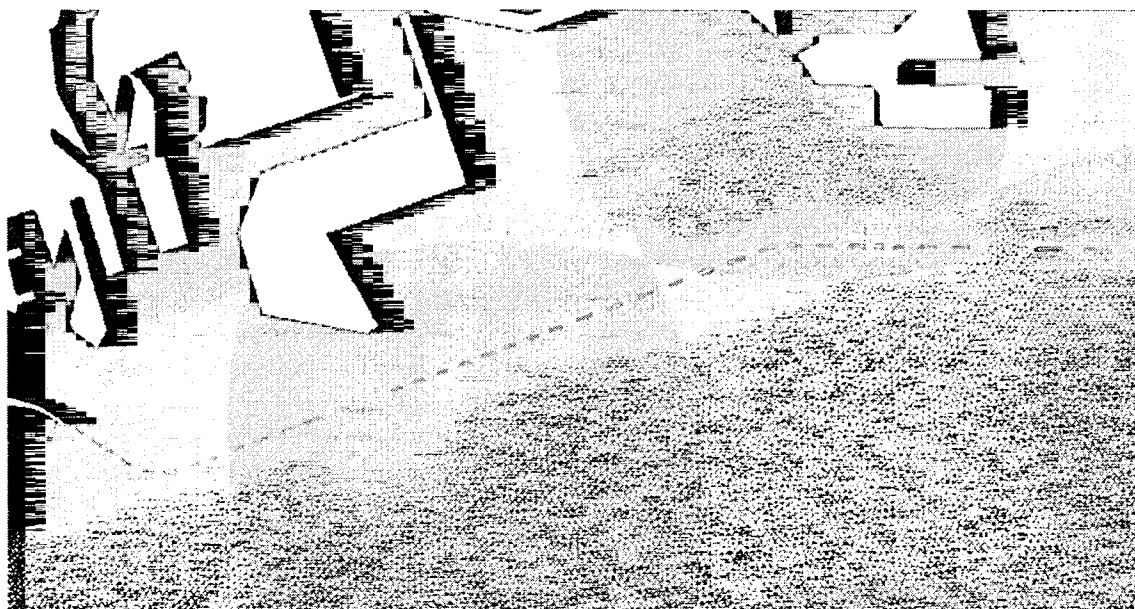


Figure 13. Diagram shows the grid for Los Angeles/Long Beach Harbor complex with 50% breakwater permeable.

Periods used by numerical model for long waves	
period band	Frequency-cps
217.01	0.004608
222.46	0.004495
230.46	0.004339
242.73	0.00412
250.46	0.003993
260.46	0.003839
275.36	0.003632
290.46	0.003443
303.46	0.003295
318.14	0.003143
335.46	0.002981
355.46	0.002813
376.64	0.002655
400.5	0.002497
430.5	0.002323
461.52	0.002167
512.46	0.001951

Table 2. Periods Used by Numerical Model for Long Waves

frequency bands stated earlier. In all, simulations were made for 10, 30, and 17 frequency components in the three bands for each incident wave angle. These components are irregularly spaced and correspond approximately to the discrete frequency components used by Seabergh and Thomas (1995) in their hydraulic model simulations. In total, 171 simulations are shown. From Table 1, we can see that, for long period waves, Seabergh and Thomas irregularly use 6 components for their experiments. But in all of our numerical simulations, to get better results, we use 17 period components for long wave band. The periods we used are listed in Table 2.

An example of the modeled resonance curve is shown in Fig. 14. At  $T = 45$  s, the lab data show a remarkably high amplification that the model underpredicts; conversely, for  $T$  between 300 s and 400 s, the numerical model value is greater than the hydraulic model data. Another example of the modeled resonance curve is shown in Fig. 15. At  $T = 45$  s and  $T = 300$  s, the laboratory data show high amplifications that the model underpredicts. The overall results for all gages, using the averaging described above, are compared against the hydraulic model data in Fig. 16. In general, the numerical simulation predicts the response at the gages as well as the hydraulic model data. The agreement is quite good for the short and medium period waves. Greater discrepancy is seen for the long waves which also exhibit greater gage-to-gage variability. For the long waves, there seems to be systematic overprediction near certain gages. These discrepancies could be attributed to several factors. First, the two bathymetry sets are not identical and the high variability

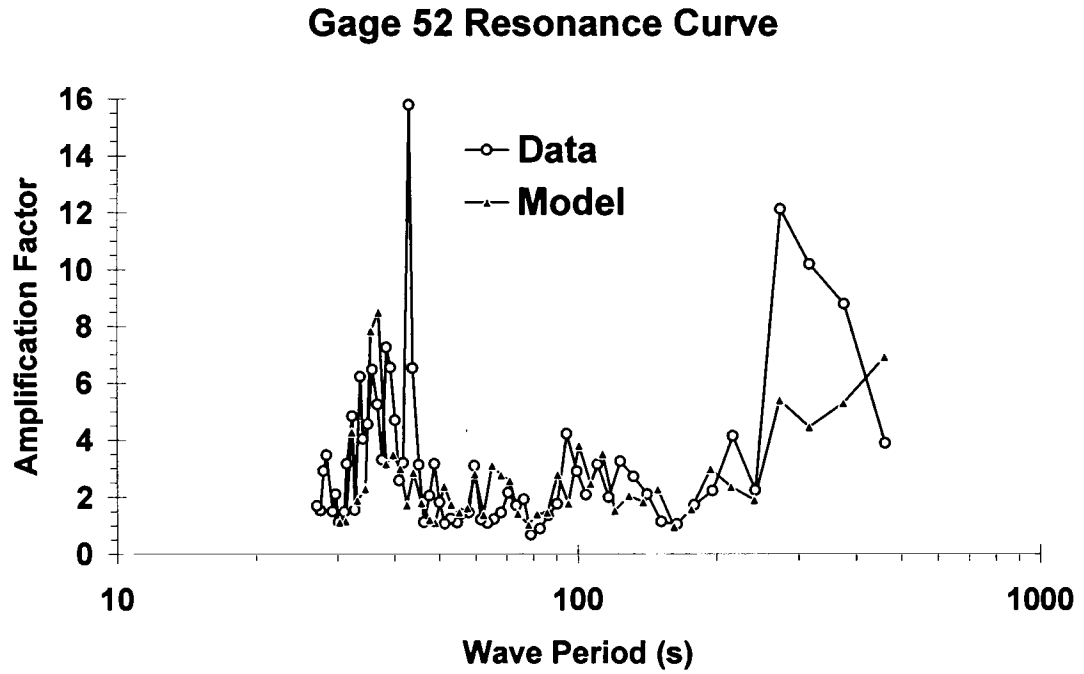


Figure 14. Resonance curve comparison at gage 52 between Numerical Model and Data (Hydraulic Model).

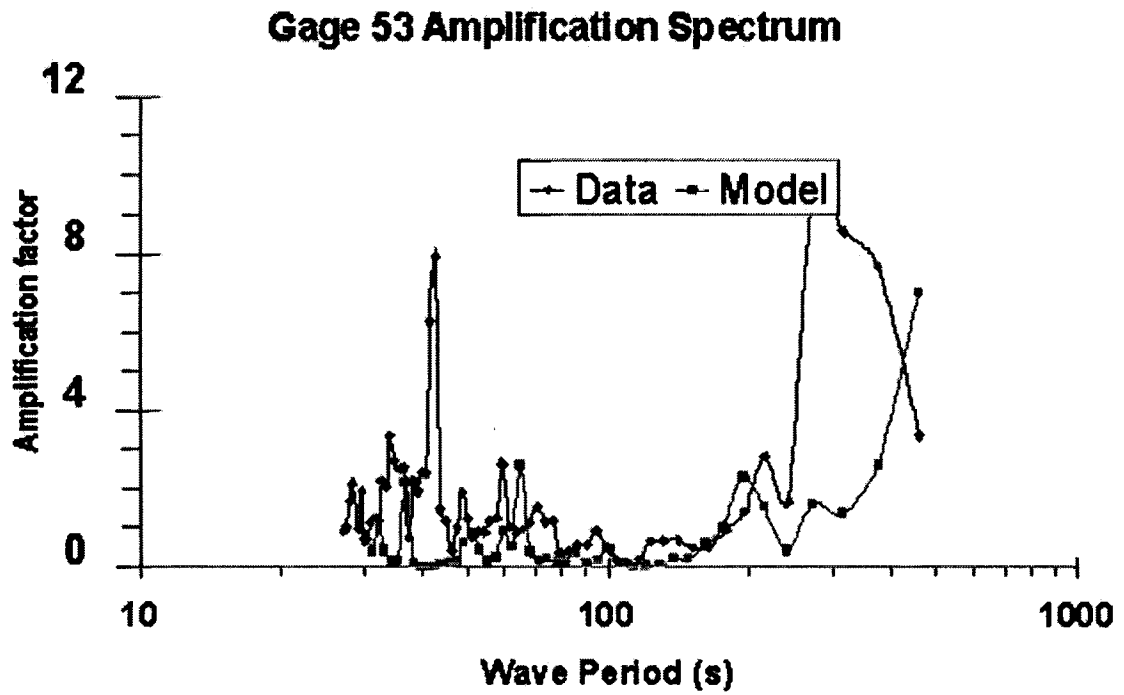


Figure 15. Resonance curve comparison at gage 53 between Numerical Model and Data (Hydraulic Model).

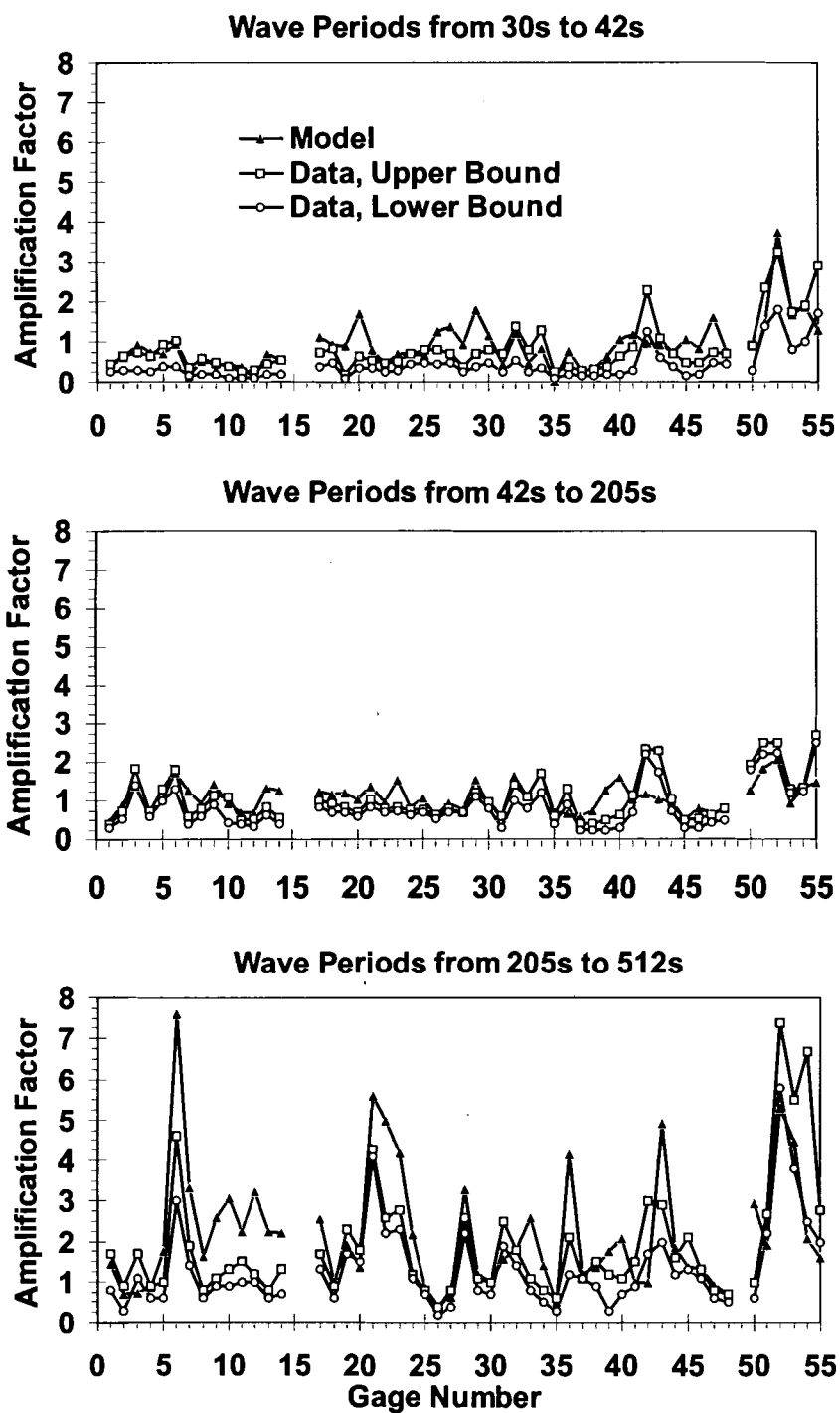


Figure 16. Comparison between Numerical Model (CGWAVE) and Lab results.

implies that small differences in the geometry can result in large differences in the response. The location of the input wave is also different in the hydraulic and numerical model. Further, the exterior sea is bounded in the hydraulic model, thus, possibly preventing radiation out to the open sea. Further, reflection coefficients and the degree of permeability of the breakwater are not sufficiently well-known. Finally, the high variability of the curves suggests that small changes can have big effects. Therefore, including “steep slope terms” in the model may improve the results (Panchang and Demirbilek, 2001).

It is of course possible to introduce dissipation and /or adjust reflection coefficients or breakwater closure to tune the model better so that a calibrated model for the Los Angeles/Long Beach complex would be available for future use. However, there is no assurance that the hydraulic model is the true benchmark. Discrepancies between hydraulic model and field data are seen in Figure 17 also. The high level of agreement between the hydraulic model and numerical model results for the short and medium period waves and the moderate agreement for the long period waves indicates that the performance of the numerical and hydraulic models are certainly compatible, although not identical.

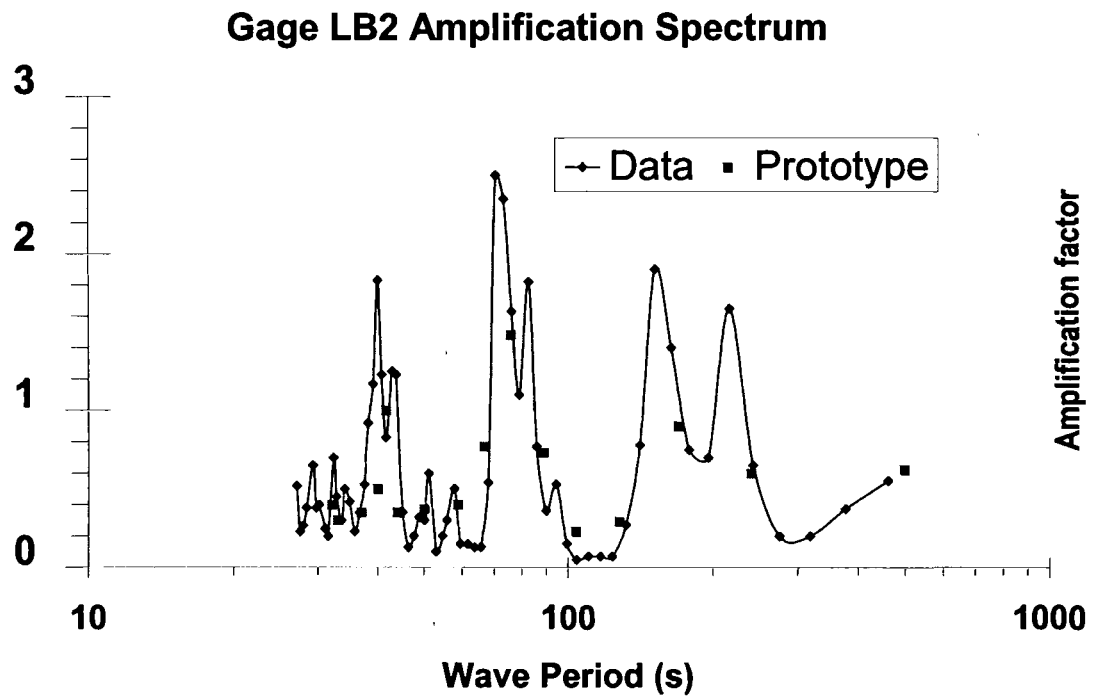


Figure 17. Resonance curve comparison at gage LB2 between Prototype and Data (Hydraulic Model).

## Chapter 5

### CONCLUSION

The most difficult problem encountered in this study is how to treat the offshore breakwaters. They are known to be permeable to waves and it is hence not appropriate to consider them as closed boundaries. In order to examine this, the numerical simulations with the full offshore breakwaters and without them were made. Comparisons between these results and the hydraulic model results are given in Figure 9 and Figure 10. Clearly, for the numerical simulations based on the bathymetric data with full breakwaters, the results are highly underpredicted. Conversely, for the numerical simulations based on the bathymetric data without any offshore breakwaters, the numerical model results are overpredicted. Permeable structures cannot be easily handled within the context of an elliptic boundary value problem. One approach may be to treat the breakwaters as a water area and ascribe an appropriate dissipation factor in that area, an alternative approach was used whereby the breakwaters was divided into several segments so that the energy could propagate through gaps in the breakwater. A decision was made to take off 50% of the breakwater. The comparison between the numerical simulations results based on this bathymetry data and the hydraulic model results were conducted. In general, the agreement is quite good for the short and medium period waves; the results are compatible for long waves.

The discrepancies could be attributed to several factors. The bathymetry data used in the hydraulic study is not available to us; we got our bathymetry data by digitizing the NOAA chart (18749). The locations of the gages used in the hydraulic study also are unknown to us; they were estimated based on Figure 1 for the numerical study. Further, the location of the input wave is also different. Also, the exterior sea is bounded in the hydraulic model; reflection coefficients and the degree of permeability of the breakwaters are not sufficiently well-known. Finally, the high variability of the curves suggests that the small changes can have big effects.

After the initial work of Chiang (1988), this effort represents the most comprehensive modeling study of wave resonance in the Los Angeles/Long Beach complex using a data set for 171 wave conditions. It was demonstrated that a state-of-the-art level wave prediction model simulates the wave climate realistically. Some of the highest amplifications occur for the longest waves (205 -512 s), with the greatest response ( $>5$ ) seen near Los Angeles Main Channel area (gage 6), West Basin area (gage 22, 35), Cerritos Channel area (gage 45), Pier J area (gage 52, 53, 54). For all other wave conditions, the amplifications are below 3. Pier J area is susceptible to high amplification even for short waves (30-42s). Consistency between two sets of results suggests that CGWAVE may be used for engineering application with the same level of confidence as a hydraulic model.

## REFERENCES

- Berkhoff, J. C. W. (1976). *Mathematical Models for Simple Harmonic Linear Water Waves. Wave Refraction and Diffraction*, Publ. 163, Delft Hydraulics Laboratory.
- Booij, N. (1981). *Gravity Waves on Water with Non-uniform Depth & Current*, Ph.D thesis, Technical Univ of Delft, The Netherlands.
- Bova, S. W., C. P. Breshears, C. Cuicchi, Z. Demirbilek, and H. A. Gabb (2000). Dual-level Parallel Analysis of Harbor Wave Response Using MPI and OpenMPI. *Internat. J. High Performance Computing Applications*. v14, 1, 49-64.
- Chen, H. S. (1990). Infinite Elements for Water Wave Radiation and Scattering. *Internat. J. Numerical Methods in Fluids*. v11, 555-569.
- Chen, H. S. and J. R. Houston (1987). Calculation of Water Level Oscillations in Harbors. *Instructional Rept. CERC-87-2*, Waterways Expt. Stn, Vicksburg, Mississippi 39180.
- Chiang, W.-L. (1988). Modelling Long and Intermediate Waves in a Harbor. *Appl. Math. Modelling*, v12, 423-428.
- Dalrymple, R. A., J. T. Kirby, and P. A. Hwang (1984). Wave Diffraction due to areas of high-energy dissipation. *J. Waterway, Port, Coastal and Ocean Engg.*, v110, No. 1, 67-79.
- Demirbilek, Z., and V. G. Panchang (1998). CGWAVE: A Coastal Surface Water Wave Model of the Mild Slope Equation, *Tech Rept CHL-98-26*, US Army Corps of Engineers Waterways Expt Stn, Vicksburg, Mississippi 39180.
- Dingemaans, M. W. (1997). *Water Wave Propagation over Uneven Bottoms*. World Scientific. Singapore.
- Ebersole, B. A. (1985). Refraction-Diffraction Model for Linear Water Wave. *J. Waterway, Port, Coastal & Ocean Engg.*, v111, No. 6. 939-953.
- Givoli, D. (1991). Non-reflecting Boundary Conditions. *J. Computat. Physics*, 94, 1-29.
- Hurdle, D. P., J. K. Kostense, and P. Bosch (1989). Mild Slope Model for the Wave Behaviour in & around Harbours and Coastal Structures. In: *Advance in Water Modelling and Measurement*. Ed. M. H. Palmer. BHRA, The Fluid Engg Centre, Cranfield, England. 307-324.

- Irons, P. (1970). A Frontal Solution Program for Finite Element Analysis. *Internatl. J. Numerical Methods Engg.*, 2, 5-32.
- Isaacson, M., and S. Qu (1990). Waves in a Harbour with Partially Reflecting Boundaries. *Coastal Engg*, v14, 193-214.
- Jones, N. L., and D. R. Richards (1992). Mesh Generation for Estuarine Flow Models. *J. Waterway, Port, Coastal and Ocean Engg.*, v118, No. 6, 3-20.
- Kirby, J. T. (1986). Higher Order Approximation in the Parabolic Equation Method for Water Waves. *J. Geophys. Research*, 91 (c1), 933-952.
- Kostense, J. K., K. L. Meijer, M. W. Dingemans, A. E. Mynett, and P. van den Bosch (1986). Wave Energy Dissipation in Arbitrarily Shaped Harbours of Variable Depth. *Proc. 20th Internat. Conf. Coastal Engg., Washington D. C.*, 2002-2016.
- Kostense, J. K., M.W. Dingemans, and P. van den Bosch (1988). Wave-Current Interaction in Harbours. *Proc. 21th Internat. Conf. Coastal Engg., ASCE, New York*, v1, 32-46.
- Lee, J. J., and F. Raichlen (1972). Oscillations in Harbors with connected basins. *J. Waterways, Harbors, and Coastal Engg Div, ASCE*. v98, 311-332.
- Lennon, G. P., P. L.-F. Liu, and J. A. Liggett (1982). Boundary Integral Solutions of Water Wave Problems. *J. Hydr. Div. ASCE*. v108, 921-931.
- Li, B. (1994a). A Generalized Conjugate Gradient Model for the Mild Slope Equation. *Coastal Engg*, 23, 215-225.
- Li, B. (1994b). An Evolution Equation for Water Waves. *Coastal Engg*, 23, 227-242.
- Li, B., and K. Anastasiou (1992). Efficient Elliptic Solvers for the Mild-Slope Equation using the Multigrid Method. *Coastal Engg*, 16, 245-266.
- Li, B., D. E. Reeve, and C. A. Fleming (1993). Numerical Solution of the Elliptic Mild-Slope Equation for Irregular Wave Propagation. *Coastal Engg*, 20, 85-100.
- Mei, C. C. (1983). *The Applied Dynamics of Ocean Surface Waves*. John Wiley, New York.
- OARB (1997). OpenMP Fortran Application Program Interface. *OpenMP Architecture Review Board (OARB) v1.0*, <http://www.openmp.org>, October 1997.

- Oliveira, F. S. B. F., and K. Anastasiou (1998). An Efficient Computational Model for Water Wave Propagation in Coastal Regions. *Applied Ocean Research*, 20, No. 3, 263-271.
- Panchang, V. G., B. Cushman-Roisin, and B. R. Pearce (1988). Combined Refraction-Diffraction of Short Waves for Large Coastal Regions. *Coastal Engg.*, v12, 133-156.
- Panchang, V. G., W. Ge, B. Cushman-Roisin, and B. R. Pearce (1991). Solution to the Mild-Slope Wave Problem by Iteration. *Applied Ocean Research*, 13, No. 4, 187-199.
- Panchang, V. G., B. Xu, and B. Cushman-Roisin. (1993). Bathymetric Variations in the Exterior Domain of a Harbor Wave Model, Proc. *Internat. Conf. on Hydroscience & Engineering, Washington DC*. 1555-1562.
- Panchang, V. G., B. Xu, and Z. Demirbilek (1999). Wave Prediction Models for Coastal Engineering Applications. Ch. 4 in: *Developments in Offshore Engineering*, Ed. J. B. Herbich. Gulf Publishing, Houston. 163-194.
- Panchang, V. G., W. Chen, B. Xu, K. Schlenker, Z. Demirbilek, and M. Okihiro (2000). Effects of Exterior Bathymetry in Elliptic Harbor Wave Models, *J. Waterway, Port, Coastal & Ocean Engg.*, v126, 2, 71-78.
- Panchang, V. G., and Z. Demirbilek (2001). Simulation of Waves in Harbors using Two-Dimensional Elliptic Equation Models. *Advances in Coastal and Ocean Engg.*, v7, 2001.
- Pos, J. D., and F. A. Kilner (1987). Breakwater Gap Wave Diffraction: An Experimental and Numerical Study. *J. Waterway, Port, Coastal, & Ocean Engg.*, v113, 1, 1-21.
- Radder, A. C. (1979). On the Parabolic Equation Method for Water-Wave Propagation. *J. Fluid Mech.*, 95, 159-176.
- Schaffer, H. A., and I. G. Jonsson (1992). Edge Waves Revisited. *Coastal Engg.*, v16, 349-368.
- Seabergh, W. C., and L. J. Thomas (1995). Los Angeles Harbor Pier 400 Harbor Resonance Model Study. US Army Corps of Engineers Waterways Expt Stn, Vicksburg, MS 39180. TR CERC-95-8.
- Smith, G. D. (1978). Numerical solution of partial differential equations: Finite Difference Methods. Oxford University Press, Oxford.

- Smith, R., and T. Sprinks (1975). Scattering of Surface Waves by a Conical Island, *Jnl. Fluid Mech*, 72, p 373.
- Thompson, E. F., H. S. Chen and L. L. Hadley (1996). Validation of Numerical Model for Wind Waves and Swell in Harbors. *J. Waterway, Port, Coastal and Ocean Engg.*, v122, 5, 245-256.
- Tsay, T.-K., and P. L.-F. Liu (1983). A Finite Element Model for Wave Refraction and Diffraction. *Applied Ocean Research*, v5, No. 1, 30-37.
- Tsay, T.-K., W. Zhu, and P. L.-F. Liu (1989). A Finite-Element Model for Wave Refraction, Diffraction, Reflection, and Dissipation. *Applied Ocean Research*, 11, 33-38.
- Xu, B., and V. G. Panchang (1993). Outgoing Boundary Conditions for Elliptic Water Wave Models. *Proceedings, The Royal Society of London, Series A*. v441, 575-588.
- Xu, B., V. G. Panchang, and Z. Demirbilek (1996). Exterior Reflections in Elliptic Harbor Wave Models. *J. Waterway, Port, Coastal and Ocean Engg.*, v122, 3, 118-126.
- YOTO (1998). "Our Ocean Future," Year of the Ocean, Themes & Issues Concerning the Nation's Stake in the Oceans. Prepared by the H. John Heinz III Center for Science, Economics, and the Environment. Office of the Chief Scientist, NOAA, Washington, DC 20230.
- Zundell, A. K., A. L. Fugal, N. L. Jones, and Z. Demirbilek (1998). Automatic Definition of Two-dimensional Coastal Finite Element Domains. In: *Hydroinformatics98, Proc. 3rd Internat. Conf. Hydroinformatics*. Ed. V. Babovic and L. C. Larsen. A. A. Balkema, Rotterdam. 693-700.

## BIOGRAPHY OF THE AUTHOR

Dongcheng Li was born in Mengzhou, Henan, People's Republic of China on August 2, 1972. He attended the public schools in Mengzhou, Henan, and was graduated from Mengzhou High School in 1991.

In September 1991, Dongcheng entered Changsha Railway University (now Central South University) at Changsha, Hunan, and in July 1995 he received his Bachelor of Mechanical Engineering degree. He served as an engineer at Taifeng Inc., Henan from 1995 to 1997.

Dongcheng enrolled for graduate study in the fall of 1997 at the University of Maine in Orono, Maine. He transferred to New Jersey Institute of Technology in January 2001. He received his Master's degree of Computer Science in May 2002. Dongcheng is a candidate for the Master of Science degree in Mechanical Engineering from The University of Maine in August 2002.